



## OPEN ACCESS

## EDITED BY

Chaojie Li,  
University of New South Wales, Australia

## REVIEWED BY

Cao Yingping,  
Hong Kong Polytechnic University, Hong Kong SAR, China  
Ling Zheng,  
Changsha University of Science and Technology, China

## \*CORRESPONDENCE

Junyu Xie,  
✉ x15823764526@163.com

RECEIVED 01 April 2024

ACCEPTED 26 April 2024

PUBLISHED 15 May 2024

## CITATION

Liu A, Li X, Li Y, Hao S, Miao Y, Zheng Y, Xie J and Yao Q (2024), Collaborative scheduling method of active-reactive power for rural distribution systems with a high proportion of renewable energy.  
*Front. Energy Res.* 12:1410694.  
doi: 10.3389/fenrg.2024.1410694

## COPYRIGHT

© 2024 Liu, Li, Li, Hao, Miao, Zheng, Xie and Yao. This is an open-access article distributed under the terms of the [Creative Commons Attribution License \(CC BY\)](https://creativecommons.org/licenses/by/4.0/). The use, distribution or reproduction in other forums is permitted, provided the original author(s) and the copyright owner(s) are credited and that the original publication in this journal is cited, in accordance with accepted academic practice. No use, distribution or reproduction is permitted which does not comply with these terms.

# Collaborative scheduling method of active-reactive power for rural distribution systems with a high proportion of renewable energy

Anjiang Liu<sup>1</sup>, Xinhao Li<sup>1</sup>, Yue Li<sup>1</sup>, Shuqing Hao<sup>1</sup>, Yu Miao<sup>1</sup>, Youzhuo Zheng<sup>1</sup>, Junyu Xie<sup>2\*</sup> and Qianqian Yao<sup>2</sup>

<sup>1</sup>Electric Power Research Institute of Guizhou Electric Power Grid Co., Ltd., Guiyang, China, <sup>2</sup>North China Electric Power University, Beijing, China

Large-scale distributed renewable energy connected to the rural distribution network has given birth to a new rural distribution system with a high proportion of new energy typical characteristics, and the optimal scheduling of the new rural distribution system has become an important issue to ensure the safe and stable operation of the power grid. This paper proposes a method of active-reactive power collaborative optimization scheduling for rural power distribution system with a high proportion of renewable energy. Firstly, the active support capability evaluation model is established, and the active power support capability and reactive power support capability of rural power distribution system are quantitatively evaluated, which provides data basis and boundary conditions for the scheduling part. Then, considering power-loss cost, distribution network operation cost, and penalty cost, a method of active-reactive power collaborative optimization scheduling for rural power distribution systems with a high proportion of renewable energy is proposed. Finally, the active support capability evaluation and regulation platform of the rural power distribution system is built to provide technical support services for the safe and stable operation of the rural power distribution system. Given the problems of overload and overvoltage faced by rural power distribution systems with a high proportion of renewable energy, this paper aims to solve the key technical challenges of optimization and regulation of new rural power distribution systems. The results show that the optimized control method proposed in this paper has better security and economy, and is conducive to promoting the construction and operation of the new rural power distribution system.

## KEYWORDS

informer model, active support capability, power forecasting, distributed resources, optimal power flow

## 1 Introduction

In 2021, the State Council issued the “2030 Carbon Peak Action Plan” and China’s power industry ushered in deepening reform (Ru et al., 2021). Traditional fossil energy is gradually replaced by clean and efficient renewable energy (Zhou et al., 2021). Rural renewable resources have great potential, which is convenient for local materials and local utilization. It is an important base for the development of new energy power generation such as rooftop photovoltaic, distributed wind power and biogas power generation

(Wu et al., 2011). The “14th Five-Year Plan for Renewable Energy” proposes the action of thousands of households and thousands of villages to control the wind, coordinate the construction of distributed photovoltaics in rural areas, vigorously promote the construction of rural wind power, and promote the construction of a new rural energy system (Fu and Zhou, 2023).

In this context, rural decentralized wind power and distributed rooftop photovoltaics have developed rapidly in recent years, and the scale has shown exponential growth (Wang et al., 2023a). The access of large-scale distributed renewable energy to the rural distribution network has spawned a new type of rural power grid with high proportion of new energy and typical characteristics of bidirectional power flow (Han et al., 2022). On the one hand, it provides more clean energy for the power system, and on the other hand, it also brings great pressure to the safe and stable operation of the power system. Due to the relatively weak rural power grid (Chawda and Shaik, 2022), a large number of distributed energy access to the rural distribution network after the overload, overvoltage, harmonic overrun, power supply quality decline and other issues (Akinyemi et al., 2022; Xu et al., 2024). Therefore, it is a great challenge to build a low-carbon, efficient, safe and stable rural energy system and form a rural power system with new energy as the main body.

Nowadays, in addition to a variety of distributed resources, more power electronic devices are also involved in power flow optimization control. The power flow controller can effectively deal with the above problems. It is connected to the distribution network in series and parallel, which can compensate the active and reactive power of the line and provide active and reactive power support for the power system. The unified power flow controller (UPFC) is the most powerful and optimal line power flow control device at present (Osama abed el-Raouf et al., 2023). It has the ability of voltage regulation and series compensation. It can not only carry out power flow regulation but also carry out harmonic control, which can effectively improve the stability of power system operation and improve the consumption rate of renewable energy (Wu et al., 2022). For example, in Reference (Albatsh et al., 2017), a shunt and series controller based on a PI and FLC UPFC prototype was used to successfully control the power flow in the transmission line, and other power system parameters were also significantly improved.

Since voltage quality is one of the important indexes to evaluate the level of power system (Kharrazi et al., 2020), how to adjust voltage quickly and effectively is an important research hotspot. Aiming at the problem of voltage instability caused by high proportion of renewable energy access to distribution network, the current control methods are divided into reactive power compensation and active power reduction. In Reference (Hou et al., 2024), a dynamic reactive power/voltage control strategy of active distribution network considering voltage stability is proposed. By reasonably controlling the action time of reactive power regulating equipment, the optimal distribution of reactive power flow in active distribution network within 1 day is realized, and the safety and stability of system operation are improved. References (Zhang et al., 2024a) considered the influence of electric vehicle access on the power grid, and proposed to use the on-load voltage regulator and electric vehicle in the distribution network for coordinated voltage regulation. In (Almeida et al., 2021;

Xiao et al., 2021), the reactive power and voltage control strategy of distribution network considering the reliability of photovoltaic power supply is proposed by using the reactive power support ability of photovoltaic power supply. In reference (Li et al., 2019), the local voltage control based on real-time measurement can quickly respond to the frequent fluctuations of distributed generation (DG). A local voltage control strategy of DG with reactive power optimization based on Kriging surrogate model is proposed. However, due to the high impedance ratio of the distribution network, there is a problem of strong coupling between active power and reactive power. Simple active or reactive power optimization scheduling is difficult to meet the safe operation and economic requirements of the distribution network, and the uncertainty of distributed power output will cause serious voltage fluctuations. Therefore, it is necessary to coordinate and optimize the active power and reactive power resources in the distribution network (Liu et al., 2022a; Jiang et al., 2023a).

The current research on active-reactive power coordinated scheduling mainly focuses on improving the efficiency and stability of power systems, especially with the high integration of renewable energy sources. This field involves a variety of technologies and methods, including optimization algorithms, prediction models, and real-time scheduling strategies. Internationally, research on active-reactive power coordinated scheduling often emphasizes integrating advanced prediction technologies and optimization algorithms to manage the uncertainty and variability of renewable energy sources (Huang et al., 2022). In terms of prediction, machine learning models such as neural networks and support vector machines are used to predict energy output (Gao et al., 2017; Zhou et al., 2019; Babbar et al., 2021; Zhuang et al., 2023), or Transformer model and Informer model for ultra-short-term prediction of wind and light (Jiang et al., 2023b; Zhang et al., 2024b; Zhuang et al., 2024). In the aspect of optimal scheduling, intelligent algorithms such as genetic algorithm and particle swarm optimization are used to optimize the scheduling. Convex programming methods such as semi-definite programming (SDP) and second-order cone programming (SOCP) can also be used to solve the problem of active-reactive power collaborative optimization (Gao et al., 2018). In China, research on active-reactive power coordinated scheduling is also actively progressing, especially against the backdrop of the national grid's intelligent upgrade. Domestic research often focuses more on the stability and security of the grid, with research teams developing customized models and algorithms that cater to the characteristics of the Chinese grid. For example, researchers explore scheduling models based on real-time monitoring and prediction, as well as optimization scheduling strategies considering the characteristics of grid loads. In general, it is of great practical significance to study the coordinated optimization of active and reactive power after the high proportion of renewable energy is connected to the grid, in order to reduce the abandonment of wind and light to improve the energy consumption capacity and improve the node voltage quality after the renewable energy is connected to the grid.

Considering the above research basis and challenges, this paper focuses on a new rural power distribution system with a high proportion of renewable energy. A method of active power and reactive power cooperative optimization control for rural power distribution system with high proportion of renewable energy is

proposed in order to provide technical support services for the safe and stable operation of rural power distribution system and promote the safe, economic and stable operation of the distribution system. The specific innovations of this paper are as follows:

1. An active support capacity evaluation model is established, and multiple indices are proposed for both active power support capacity and reactive power support capacity, in order to systematically assess the overall active support capacity of rural power distribution systems with a high proportion of renewable energy. This provides the data basis and boundary conditions for the scheduling part.
2. Comprehensively considering the operation characteristics of multiple distributed resources and power flow controllers, a method of active-reactive power collaborative optimization scheduling for rural power distribution system with high proportion of renewable energy is proposed to minimize power-loss cost, distribution network operation cost, and penalty cost.
3. The active support capability evaluation and regulation platform of the rural power distribution system is built. By accessing the real-time operation data of distributed resources, the active support capability evaluation of distributed resources and the scheduling control function of the new rural power distribution system is realized, and technical support services are provided for the safe and stable operation of the rural power distribution system.

## 2 Active support capability evaluation model

Active support capability evaluation is very important for the safe and stable operation of rural power distribution system, which can show the adjustment ability of distributed photovoltaic power generation equipment when the system voltage and power flow fluctuate. The evaluation part is divided into active power support capability evaluation and reactive power support capability evaluation. The active power/reactive power adjustable capability of photovoltaic is quantitatively evaluated, which is used as the data support and boundary conditions of the subsequent scheduling part.

### 2.1 Assessment of active power support capability

#### 2.1.1 Informer model

The power load and photovoltaic output in rural distribution networks have obvious time series characteristics. The Informer model is introduced into the time series prediction problem to capture time series characteristics with its strong time series prediction ability. The Informer model is improved on the Transformer model by introducing the multi-head ProbSparse self-attention mechanism and the self-attention distillation mechanism, effectively reducing computational complexity. On this basis, by using a generative decoder, all prediction results can be generated at once, further improving computational efficiency. The Informer model consists of two parts: Encoder

and Decoder, as depicted in Figure 1. The input time series information is encoded as a hidden state representation in the Encoder and decoded in the Decoder section to output predicted values. The specific principle is as follows:

The Encoder consists of the multi-head ProbSparse self-attention mechanism and the self-attention distillation mechanism, which extracts data features from time series. By using the multi-head ProbSparse self-attention mechanism, the computational complexity is effectively reduced. The calculation formula can be expressed as Eq. 1,

$$\text{Attention}(Q, K, V) = \text{Soft max}\left(\frac{\bar{Q}K^T}{\sqrt{d}}\right)V \quad (1)$$

Where Softmax is an activation function;  $Q, K, V \in C^{N \times d}$  respectively represent the query matrix, key matrix, and value matrix, which are obtained by combining the input feature vectors with the corresponding weighted matrix;  $\bar{Q}$  is the query matrix obtained by sparse calculation of matrix  $Q$ ;  $d$  and  $N$  represent the input dimension and variable dimension, respectively.

Then, the self-attention distillation mechanism is used to reduce network complexity and highlight features, greatly enhancing the processing ability for time series. The operating formula for distillation from the  $l$  layer to the  $l+1$  layer is shown in the equation as Eq. 2,

$$x_t^{l+1} = \text{MaxPool}\left(\text{ELU}\left(\text{Convld}\left([x_t^l]_{AB}\right)\right)\right) \quad (2)$$

Where  $x_t^l$  represents the input of layer  $l$  at time  $t$ ;  $[\cdot]_{AB}$  and Convld represent the operations of multi-head ProbSparse self-attention mechanism and one-dimensional convolution operations, respectively; ELU and MaxPool represent activation functions and max pooling operations, respectively.

The Decoder consists of the multi-head ProbSparse self-attention mechanism, multi-head attention mechanism, and a fully connected layer, which can obtain all time series prediction results at once.

This article uses the maximum mutual information coefficient method to filter relevant meteorological data and historical sequence data as inputs to the Informer model, and then predict the active power  $P_{i,t}^{Load}$  and reactive power  $Q_{i,t}^{Load}$  of node loads and the active power  $P_{i,t}^{PV}$  of photovoltaic for a total of 96 time points in the next 24 h.

#### 2.1.2 Evaluation indicators for active power support capacity

The active power support capacity of rural distribution systems is usually composed of electricity consumption level and power generation level. Therefore, this article proposes evaluation indicators for distributed resources and power load in rural distribution systems to measure the active power support capacity within the distribution area.

Based on the Informer model, interval and point predictions were made for the photovoltaic output and power load of rural distribution systems, obtaining data on upper and lower limits and prediction results for 96 continuous time nodes, respectively. Then, two indicators, maximum/minimum range and maximum fluctuation range are proposed as evaluation criteria for the active power support capability. Among them, the maximum/

minimum range represents the maximum/minimum difference between the upper and lower limits of the interval prediction results, which represents the maximum/minimum amplitude of data fluctuation within the specified time. The maximum fluctuation range is the value of the first-order derivative of the point prediction result, used to represent the stability of the data within the specified time.

All in all, this section presents an evaluation method of active power support capability, which includes prediction and evaluation. The part of prediction forecasts the active and reactive power of photovoltaics and load nodes based on the Informer model, and these data will be used in the scheduling part as input data, while the results of the active power support capability evaluation part will be used as the boundary conditions of active power related constraints.

## 2.2 Assessment of reactive power support capability

Compared to regulating active power, reactive power regulation has a smaller impact on the user's profits and lower regulation costs. Therefore, reactive power regulation is generally chosen as the voltage regulation method. This article takes the voltage support degree and reactive power regulation capacity as evaluation indicators to measure the reactive power support ability of nodes where distributed resources are located.

### 2.2.1 Voltage support degree

The voltage support degree represents the degree to which the voltage of the regional power grid is affected by changes in the reactive power of distributed resources. The approximate linear relationship between node power injection and voltage amplitude change can be represented by the definitions of active voltage sensitivity and reactive voltage sensitivity as Eqs 3, 4:

$$S_{i,j,t}^P = \frac{\Delta U_{i,t}}{\Delta P_{i,t}} \quad (3)$$

$$S_{i,j,t}^Q = \frac{\Delta U_{i,t}}{\Delta Q_{i,t}} \quad (4)$$

Where  $\Delta U_{i,t}$ ,  $\Delta P_{i,t}$  and  $\Delta Q_{i,t}$  respectively represent the changes of voltage amplitude, active power, and reactive power of node  $i$  at time  $t$ ;  $S_{i,j,t}^P/S_{i,j,t}^Q$  is the active/reactive-voltage sensitivity coefficient, which can be obtained from the modified equation of the power flow calculation, it represents the voltage change at node  $i$  at time  $t$  when the unit of active/reactive power changes at node  $j$ .

The power flow sensitivity analysis method is used to linearize the current operating point of the power grid, and then approximate the voltage changes at each node during the voltage regulation process through active voltage sensitivity and reactive voltage sensitivity as shown in Eq. 5,

$$\begin{bmatrix} \Delta U_{1,t} \\ \Delta U_{2,t} \\ \vdots \\ \Delta U_{N,t} \end{bmatrix} = \begin{bmatrix} S_{1,1,t}^P & \dots & S_{1,M,t}^P \\ \vdots & \ddots & \vdots \\ S_{N,1,t}^P & \dots & S_{N,M,t}^P \end{bmatrix} \begin{bmatrix} \Delta P_{1,t} \\ \Delta P_{2,t} \\ \vdots \\ \Delta P_{M,t} \end{bmatrix} + \begin{bmatrix} S_{1,1,t}^Q & \dots & S_{1,M,t}^Q \\ \vdots & \ddots & \vdots \\ S_{N,1,t}^Q & \dots & S_{N,M,t}^Q \end{bmatrix} \begin{bmatrix} \Delta Q_{1,t} \\ \Delta Q_{2,t} \\ \vdots \\ \Delta Q_{M,t} \end{bmatrix} \quad (5)$$

Where  $N$  and  $M$  represent the total number of nodes and the number of connected photovoltaics in the rural distribution network, respectively.

### 2.2.2 Reactive power regulation capacity

The reactive power regulation capability of photovoltaics is affected by the capacity of grid-connected inverters. When the active power of photovoltaics does not change, grid-connected inverters need to meet capacity constraints as Eq. 6,

$$\sqrt{(P_{i,t}^{PV})^2 + (Q_{i,t}^{PV} + \Delta Q_{i,t}^{PV})^2} \leq S_i^{PV} \quad (6)$$

Where  $P_{i,t}^{PV}$  and  $Q_{i,t}^{PV}$  respectively represent the initial active power and reactive power of the photovoltaic at node  $i$  at time  $t$ ;  $S_i^{PV}$  indicates the capacity of the photovoltaic grid-connected inverter at node  $i$ . Therefore, the upper and lower limits of reactive power regulation of photovoltaic at node  $i$  at time  $t$  can be expressed as follows,

$$\Delta Q_{i,t,\max}^{PV} = \sqrt{(S_i^{PV})^2 - (P_{i,t}^{PV})^2} - Q_{i,t}^{PV} \quad (7)$$

$$\Delta Q_{i,t,\min}^{PV} = -\sqrt{(S_i^{PV})^2 - (P_{i,t}^{PV})^2} - Q_{i,t}^{PV} \quad (8)$$

Due to the influence of node load, photovoltaic output, and photovoltaic grid-connected inverter capacity in the distribution network, the reactive power regulation ability of different node photovoltaics will undergo significant changes. Eqs 7, 8 can accurately represent the reactive power adjustable capacity of the photovoltaic without affecting the comparison of the reactive power adjustable capacity between nodes. The difference in the adjustable capacity only depends on the initial reactive power output of the photovoltaic. Therefore, the upper limit of reactive power adjustment of the photovoltaic can be selected as the indicator of reactive power adjustment capacity.

Consequently, a reactive power support capability evaluation method is proposed in this section, which quantifies the reactive power support capability of distributed resources to the rural power distribution system. By the way, the results of the voltage support degree part will be used as a reference for the reactive power adjustment of the scheduling part, and the results of the reactive power regulation capacity part will be used as the boundary conditions of reactive power related constraints.

## 3 Active-reactive power collaborative optimization scheduling

This section utilizes the load and photovoltaic time series data predicted based on the Informer model in Section 2, as well as the evaluation results of active support capability, to carry out the active-reactive power collaborative optimization scheduling of rural distribution systems at the daily level.

### 3.1 Optimization objective

With the development of rural distribution systems and the improvement of demand response awareness, demand-side

resources are becoming increasingly diversified. The active-reactive power collaborative optimization scheduling of rural distribution systems can be expressed as a multi-objective optimization scheduling model that comprehensively considers power loss, operating costs, and system demand response in the distribution network. Specifically, the optimization objectives of rural power distribution systems take into account the minimization of power-loss cost  $f_1$ , distribution network operation cost  $f_2$ , and penalty cost  $f_3$  for system demand response, as shown in Eqs 9–14,

$$f_1 = \min \sum_{t \in T} \sum_{i=1}^{nbus} \sum_{j=1}^{nbus} G_{ij,t} (V_{i,t}^2 + V_{j,t}^2 - 2V_{i,t}V_{j,t} \cos \theta_{ij,t}) \quad (9)$$

Where  $G_{ij,t}$  is the conductivity of line  $ij$  at time  $t$ ;  $V_{i,t}$  indicates the voltage amplitude of node  $i$  at time  $t$ ;  $\theta_{ij,t}$  is the phase angle of line  $ij$  at time  $t$ ;  $T$  and  $nbus$  respectively represent the number of time periods and nodes divided.

$$f_2 = \min \sum_{t \in T} \left( \sum_{i \in \Omega_{PV}} C_{i,t}^{PV} + \sum_{i \in \Omega_{ES}} C_{i,t}^{ES} + \sum_{i \in \Omega_{OPQ}} C_{i,t}^{CPQ} \right) \quad (10)$$

$$C_{i,t}^{PV} = \rho^{PV} \cdot P_{i,t}^{PV} = \rho^{PV} \cdot (P_{0,i,t}^{PV} - \Delta P_{i,t}^{PV}) \quad (11)$$

$$C_{i,t}^{ES} = \rho^{ES} \cdot P_{i,t}^{ES} \quad (12)$$

$$C_{i,t}^{CPQ} = \rho^{CPQ} \cdot P_{i,t}^{CPQ} \quad (13)$$

Where  $C_{i,t}^{PV}$ ,  $C_{i,t}^{ES}$  and  $C_{i,t}^{CPQ}$  represent the cost of photovoltaic power generation, energy storage operation, and regulation cost of power flow controllers, respectively;  $\rho^{PV}$ ,  $\rho^{ES}$  and  $\rho^{CPQ}$  represent the unit cost of photovoltaic power generation, the unit operating cost of energy storage, and the unit regulation cost of power flow controllers, respectively;  $P_{i,t}^{PV}$  is the active photovoltaic output at node  $i$  at time  $t$ ,  $P_{0,i,t}^{PV}$  is the active photovoltaic output before adjustment at node  $i$  at time  $t$ ,  $\Delta P_{i,t}^{PV}$  is the reduction in active photovoltaic output at node  $i$  at time  $t$ ,  $P_{i,t}^{ES}$  is the active energy storage output at node  $i$  at time  $t$ , and  $P_{i,t}^{CPQ}$  is the active power regulation of the power flow controller at node  $i$  at time  $t$ ;  $\Omega_{PV}$ ,  $\Omega_{ES}$  and  $\Omega_{CPQ}$  are the sets of nodes connected to photovoltaic, energy storage, and power flow controllers, respectively.

$$f_3 = \min \sum_{t \in T} \left( \sum_{i \in \Omega_{OPQ}} |P_{i,t}^{CPQ}| \cdot \lambda_t^{CPQ} + \sum_{i \in \Omega_{EV}} |P_{i,t}^{EV}| \cdot \lambda_t^{EV} \right) \quad (14)$$

Where  $\Omega_{EV}$  represents the set of nodes connected to the electric vehicle load;  $P_{i,t}^{EV}$  is the adjustment amount of electric vehicle load at node  $i$  at time  $t$ ;  $\lambda_t^{PV}$ ,  $\lambda_t^{CPQ}$  and  $\lambda_t^{EV}$  represent the penalty price for photovoltaic curtailment, the degradation cost of the power flow controller's lifespan, and the compensation price for adjusting the load of electric vehicles at time  $t$ , respectively.

## 3.2 Constraint condition

### 3.2.1 Power flow and voltage constraints

This article uses the polar coordinate form of the Newton-Raphson method to represent the power flow equation in rural distribution systems, as shown in Eq. 15, while also satisfying the

balance of active and reactive power of the line shown in Eq. 16 and the voltage amplitude constraint shown in Eq. 17.

$$\begin{cases} \Delta P_{i,t}^{nbus} - \sum_{j \in L(i)}^{nbus} V_{i,t}V_{j,t} (G_{ij} \cos \theta_{ij,t} + B_{ij} \sin \theta_{ij,t}) = 0 \\ \Delta Q_{i,t}^{nbus} - \sum_{j \in L(i)}^{nbus} V_{i,t}V_{j,t} (G_{ij} \sin \theta_{ij,t} - B_{ij} \cos \theta_{ij,t}) = 0 \end{cases} \quad (15)$$

$$\begin{cases} \Delta P_{i,t} = P_{i,t}^{PV} + P_{i,t}^{ES} - P_{i,t}^{EV} - P_{i,t}^{Load} \\ \Delta Q_{i,t} = Q_{i,t}^{PV} + Q_{i,t}^{ES} - Q_{i,t}^{Load} \end{cases} \quad (16)$$

$$V_{i,t,min} \leq V_{i,t} \leq V_{i,t,max} \quad (17)$$

Where  $\Delta P_{i,t}^{nbus}$  and  $\Delta Q_{i,t}^{nbus}$  are the active and reactive power injected by node  $i$  at time  $t$ , respectively;  $P_{i,t}^{Load}$  and  $Q_{i,t}^{Load}$  are the active and reactive power consumed by node  $i$  at time  $t$ , respectively;  $L(i)$  represents the set of nodes connected to node  $i$ .

### 3.2.2 Photovoltaic constraints

Distributed photovoltaics can regulate active and reactive power output, and their regulation capacity is affected by grid-connected inverters. Based on the reactive power support evaluation results in Section 2.2, the relevant constraints of distributed photovoltaics are as Eqs 18–22,

$$(P_{i,t}^{PV})^2 + (Q_{i,t}^{PV})^2 \leq (S_i^{PV})^2 \quad (18)$$

$$0 \leq P_{i,t}^{PV} \leq P_{i,t,max}^{PV} \quad (19)$$

$$0 \leq Q_{i,t}^{PV} \leq Q_{i,t,max}^{PV} \quad (20)$$

$$0 \leq \Delta P_{i,t}^{PV} \leq \Delta P_{i,t,max}^{PV} \quad (21)$$

$$\Delta Q_{i,t,min}^{PV} \leq \Delta Q_{i,t}^{PV} \leq \Delta Q_{i,t,max}^{PV} \quad (22)$$

Where  $P_{i,t,max}^{PV}$  and  $Q_{i,t,max}^{PV}$  represent the upper limits of photovoltaic active and reactive power output, respectively;  $\Delta P_{i,t,max}^{PV}$  and  $\Delta Q_{i,t,max}^{PV}$  are the upper limits of active and reactive power reduction in photovoltaics, respectively.

### 3.2.3 Power flow controller constraints

The power flow controller is a flexible AC transmission device with superior characteristics, which can simultaneously and efficiently control the active and reactive power in the distribution network lines, and also reduce line power loss. Its constraints are as Eqs 23–25,

$$(P_{i,t}^{CPQ})^2 + (Q_{i,t}^{CPQ})^2 \leq (S_i^{CPQ})^2 \quad (23)$$

$$0 \leq P_{i,t}^{CPQ} \leq P_{i,t,max}^{CPQ} \quad (24)$$

$$0 \leq Q_{i,t}^{CPQ} \leq Q_{i,t,max}^{CPQ} \quad (25)$$

Where  $P_{i,t,max}^{CPQ}$  and  $Q_{i,t,max}^{CPQ}$  respectively represent the upper limits of active and reactive power that the power flow controller can regulate;  $S_i^{CPQ}$  represents the capacity of the power flow controller.

### 3.2.4 Energy storage constraints

Energy storage devices can balance the power flow of rural distribution systems through charging/discharging, and improve the reliability and stability of system operation. The constraints are as Eqs 26–30,

$$(P_{i,t}^{ES})^2 + (Q_{i,t}^{ES})^2 \leq (S_i^{ES})^2 \quad (26)$$

$$P_{i,t,ch,min}^{ES} \leq P_{i,t,ch}^{ES} \leq P_{i,t,ch,max}^{ES} \quad (27)$$

$$P_{i,t,dis,min}^{ES} \leq P_{i,t,dis}^{ES} \leq P_{i,t,dis,max}^{ES} \quad (28)$$

$$E_{i,t,soc}^{ES} + P_{i,t,ch}^{ES} \eta_{ch}^{ES} \Delta t - \frac{P_{i,t,dis}^{ES}}{\eta_{dis}^{ES}} \Delta t = E_{i,t+1,soc}^{ES} \quad (29)$$

$$E_{i,t,soc,min}^{ES} \leq E_{i,t,soc}^{ES} \leq E_{i,t,soc,max}^{ES} \quad (30)$$

Where  $P_{i,t,ch}^{ES}$  and  $P_{i,t,dis}^{ES}$  respectively represent the charging and discharging power of the energy storage device;  $P_{i,t,ch,min}^{ES}/P_{i,t,ch,max}^{ES}$  and  $P_{i,t,dis,min}^{ES}/P_{i,t,dis,max}^{ES}$  indicate the minimum/maximum charging and discharging power of the energy storage device, respectively;  $S_i^{ES}$  represents the capacity of the energy storage device;  $E_{i,t,SOC}^{ES}$ ,  $E_{i,t,SOC,min}^{ES}$  and  $E_{i,t,SOC,max}^{ES}$  are the stored energy and the upper and lower limits of the storage capacity of the energy storage device, respectively;  $\eta_{ch}^{ES}$  and  $\eta_{dis}^{ES}$  respectively represent the charging and discharging efficiency of energy storage devices.

### 3.2.5 Electric vehicle load constraints

The load of electric vehicles can participate in the demand side response of the distribution system under reasonable regulation strategies. Through its charging/discharging characteristics after connecting to the power grid, it can achieve bidirectional interaction with the power grid, achieve peak shaving and valley filling, and obtain certain economic compensation costs. The constraints are as Eqs 31–34.

$$P_{i,t,ch,min}^{EV} \leq P_{i,t,ch}^{EV} \leq P_{i,t,ch,max}^{EV} \quad (31)$$

$$P_{i,t,dis,min}^{EV} \leq P_{i,t,dis}^{EV} \leq P_{i,t,dis,max}^{EV} \quad (32)$$

$$E_{i,t,soc,min}^{EV} \leq E_{i,t,soc}^{EV} \leq E_{i,t,soc,max}^{EV} \quad (33)$$

$$E_{i,t,soc}^{EV} + P_{i,t,ch}^{EV} \eta_{ch}^{EV} \Delta t - \frac{P_{i,t,dis}^{EV}}{\eta_{dis}^{EV}} \Delta t = E_{i,t+1,soc}^{EV} \quad (34)$$

Where  $P_{i,t,ch}^{EV}$  and  $P_{i,t,dis}^{EV}$  respectively represent the charging and discharging power of the electric vehicle load;  $P_{i,t,ch,min}^{EV}/P_{i,t,ch,max}^{EV}$  and  $P_{i,t,dis,min}^{EV}/P_{i,t,dis,max}^{EV}$  indicate the minimum/maximum charging and discharging power of the electric vehicle load, respectively;  $E_{i,t,SOC}^{EV}$ ,  $E_{i,t,SOC,min}^{EV}$  and  $E_{i,t,SOC,max}^{EV}$  are the stored energy and the upper and lower limits of the storage capacity of the electric vehicle loads;  $\eta_{ch}^{EV}$  and  $\eta_{dis}^{EV}$  represent the charging and discharging efficiency of electric vehicle loads, respectively.

### 3.3 Solution methodology

The power flow equation in the polar coordinate form shown in Eq. 15 and the power-loss cost  $f_1$  in the comprehensive objective function have nonlinearity and non-convexity, which greatly increases the computational difficulty and complexity of optimization problems. Therefore, this paper uses the second-order cone-based branch flow method, introducing intermediate variables  $X_{i,t}$ ,  $Y_{i,j,t}$  and  $Z_{i,j,t}$  to transform the original problem into a linear cone model that is easy to solve, while ensuring solution accuracy, as shown in Eqs 35–40,

$$X_{i,t} = (V_{i,t})^2 \quad (35)$$

$$Y_{i,j,t} = V_{i,t} V_{j,t} \cos \theta_{ij,t} \quad (36)$$

$$Z_{i,j,t} = V_{i,t} V_{j,t} \sin \theta_{ij,t} \quad (37)$$

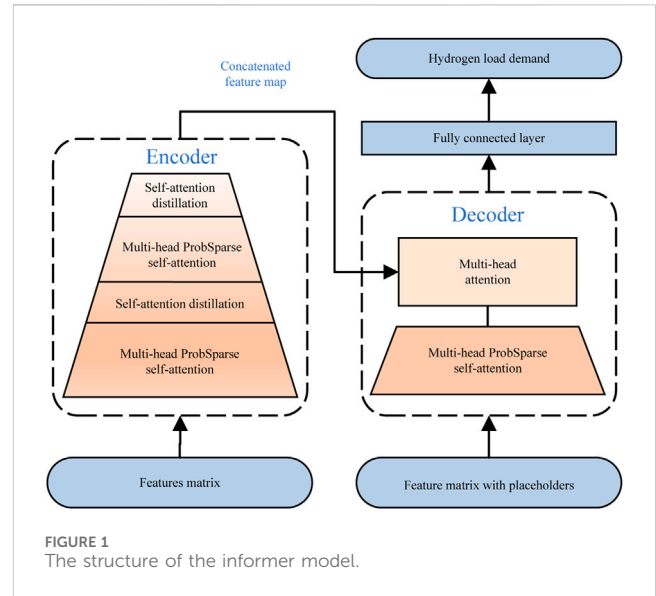


FIGURE 1 The structure of the informer model.

$$X_{i,t} X_{j,t} = (Y_{i,j,t})^2 + (Z_{i,j,t})^2 \quad (38)$$

$$M_{i,j,t} = \frac{X_{i,t} + X_{j,t}}{2} \quad (39)$$

$$N_{i,j,t} = \frac{X_{i,t} - X_{j,t}}{2} \quad (40)$$

The power-loss cost  $f_1$  Eq. 8, the power flow equation constraint in polar coordinate form Eq. 15, and the voltage amplitude constraint Eq. 17 can be transformed into the following forms, as shown in Eqs 41–43,

$$f_1 = \min \sum_{t \in T} \sum_{i=1}^{nbus} \sum_{j=1}^{nbus} G_{ij,t} (X_{i,t} + X_{j,t} - 2Y_{i,j,t}) \quad (41)$$

$$\begin{cases} \Delta P_{i,t}^{nbus} - \left( G_{ii} X_{i,t} + \sum_{j \in L(i)}^{nbus} (G_{ij} Y_{i,j,t} + B_{ij} Z_{i,j,t}) \right) = 0 \\ \Delta Q_{i,t}^{nbus} - \left( -B_{ii} X_{i,t} - \sum_{j \in L(i)}^{nbus} (B_{ij} Y_{i,j,t} - G_{ij} Z_{i,j,t}) \right) = 0 \end{cases} \quad (42)$$

$$(V_{i,t,min})^2 \leq X_{i,t} \leq (V_{i,t,max})^2 \quad (43)$$

When solving mixed-integer second-order cone programming problems, the original problem has been transformed into a polyhedral approximation of the second-order cone. When solving, Eq. 38 is relaxed and transformed into a cone constraint as shown in Eqs 44–47. At this time, the original nonconvex feasible domain is relaxed into a convex second-order cone feasible domain, which can be solved quickly and efficiently using commercial solvers such as Gurobi.

$$X_{i,t} X_{j,t} \geq (Y_{i,j,t})^2 + (Z_{i,j,t})^2 \quad (44)$$

$$\sqrt{(Y_{i,j,t})^2 + (Z_{i,j,t})^2 + (N_{i,j,t})^2} \leq M_{i,j,t} \quad (45)$$

$$\sqrt{(Y_{i,j,t})^2 + (Z_{i,j,t})^2} \leq Y_{i,j,t} \quad (46)$$

$$\sqrt{(Y_{i,j,t})^2 + (N_{i,j,t})^2} \leq M_{i,j,t} \quad (47)$$

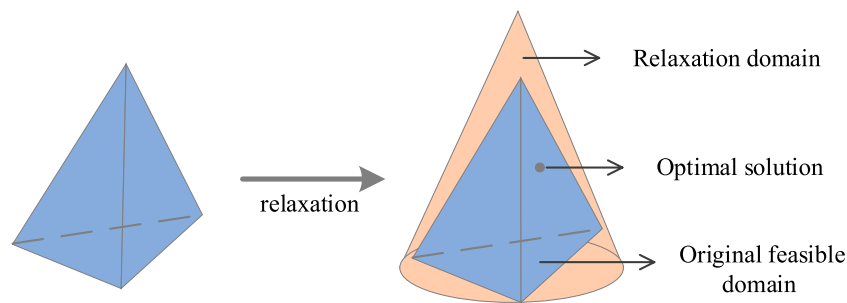


FIGURE 2  
Second-order cone relaxation principle.

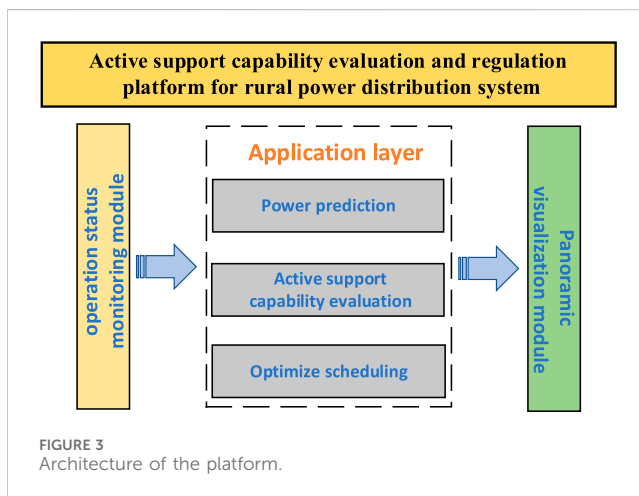


FIGURE 3  
Architecture of the platform.

As depicted in Figure 2, when considering all feasible solutions within the non-convex feasible domain are in the second-order cone plane, relaxation expands this feasible domain into convex cones. Consequently, the optimal solution to the original problem lies in the solution within the convex second-order cone and the original feasible domain.

## 4 Active support capability evaluation and regulation platform for rural power distribution system

The active support capability evaluation and regulation platform for rural power distribution system is based on database management software and software support platform, which realizes the monitoring and regulation of the operation status of rural power distribution system, as depicted in Figure 3. By accessing real-time operation data of distributed resources such as photovoltaic, energy storage, and electric vehicle loads, it realizes the active support capability evaluation of distributed resources and the scheduling and control function of the new power distribution system, providing technical support services for the safe and stable operation of rural power distribution system.

### 4.1 Operation status monitoring and panoramic visualization module

The operation status monitoring module mainly includes data collection and analysis processing, event and alarm processing, microgrid data access and control, and terminal data monitoring functions, providing data support and abnormal alarm services for the application layer. The processed data is transmitted to the application layer for simulation analysis and calculation.

The panoramic visualization module mainly involves real-time data display, including a list of display devices for the application layer's three modules, and displays the corresponding measurement/calculation data types of the devices. According to the selection, the calculated predicted/scheduled photovoltaic data information, node load information, calculation evaluation indicators, and other data curves will be displayed in real-time.

### 4.2 Application layer

The application layer consists of three modules: distributed resource power prediction, active support capability evaluation, and optimization scheduling control. Among them, the distributed resource power prediction module receives historical time series data information on distributed photovoltaic, adjustable load, and net load from the operation status monitoring module, effectively predicting future distributed photovoltaic output and user load demand.

The optimization scheduling control module involves the coordinated optimization and control of active-reactive power in rural distribution systems. It targets multiple types of distributed resources composed of distributed photovoltaics, energy storage, controllable loads, etc. (Wang et al., 2023b), and uses the output data of the distributed resource power prediction module as input to execute the active-reactive power collaborative optimization scheduling algorithm. It reasonably cooperates to optimize the active and reactive power of rural distribution systems, reduce the impact of renewable energy fluctuations and uncertainties on the operation of rural distribution networks under high penetration rates, improve power quality, and ensure the reliable and stable operation of the power grid.

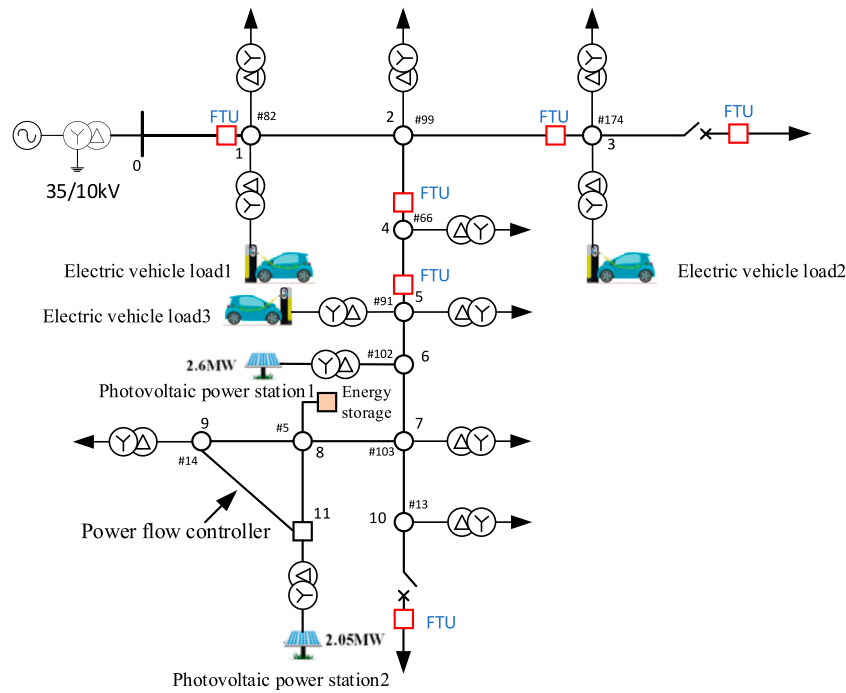


FIGURE 4  
Topology of the 11-node distribution network.

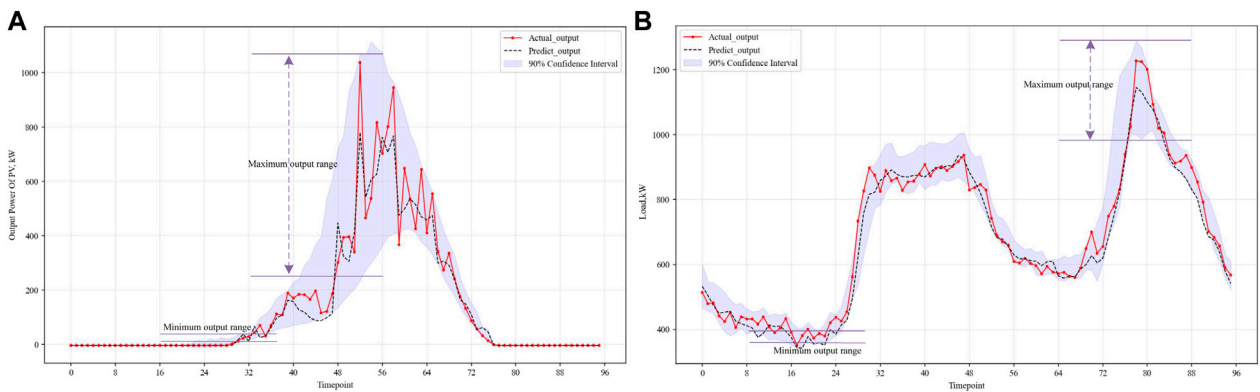


FIGURE 5  
Prediction result presentation.

The active support capability evaluation module is divided into the active power support capability evaluation model and the reactive power support capability evaluation model. The active power support capability evaluation model based on predicted data information, calculates the evaluation index formula according to the active power support capacity evaluation model proposed in Section 2.1 and then evaluates the active power support capacity of distributed resources within the region for the overall rural power distribution system. According to the reactive power support capability evaluation model proposed in Section 2.2, the reactive power support capability evaluation model is based on the

capacity of grid-connected converters of distributed resources, the predicted active power of distributed resources and user load, evaluates the upper and lower limits of voltage adjustment capacity for each distributed resource under active-reactive power collaborative optimization scheduling algorithm, and then, based on the active voltage sensitivity and reactive voltage sensitivity matrices of the system, calculate and evaluate the voltage support degree of each distributed resource node for each node in the rural distribution system, and complete the evaluation of the overall reactive power support capacity of the distributed resources in the region for the rural distribution system.



TABLE 1 Predicted fluctuation indicators.

PV			Load		
Maximum fluctuation range	Minimum fluctuation range	Maximum fluctuation amplitude	Maximum fluctuation range	Minimum fluctuation range	Maximum fluctuation amplitude
833.5518	0.3983	364.6809	400.5810	36.7028	133.2695
197.1246	0.6176	91.4882	288.9592	0.3379	133.2501
390.6840	0.0379	116.1601	99.5663	0.8750	108.5016
327.3329	27.5622	60.1674	196.1139	0.1880	103.8253
307.4116	0.1302	106.3608	265.3143	0.2697	117.4270
698.5962	0.5087	193.2312	262.1948	12.7294	141.5460
214.7788	0.5324	178.6859	411.8258	44.5950	153.2775
211.7816	0.2008	153.9651	306.7773	46.2228	124.0258
948.6616	15.5817	209.9706	326.2993	4.2378	128.4183
639.5231	1.4247	103.8170	174.1690	0.4785	114.6069
264.1783	29.0681	46.2188	135.2690	5.4687	118.9498
823.0273	0.2206	169.2849	205.8177	0.3227	111.7306
145.3241	0.1422	40.1902	311.4124	17.1906	120.6279
501.2705	0.3715	96.7539	179.0178	2.0235	139.7288
216.5244	0.2344	90.0313	205.4618	0.3065	105.7739
129.8710	21.1172	89.6522	251.2050	0.1353	103.0788
373.1213	19.0373	150.6621	210.0157	0.5725	116.2219
815.1910	0.0513	188.5215	290.8798	5.1402	115.4104

TABLE 2 Comparison of prediction accuracy.

Prediction model		Point prediction		Interval prediction	
Evaluation index		RMSE	MAE	PIPC	PINAW
PV	Informer	135.2468	76.8952	0.6779	0.0398
	Transformer	156.3272	88.9532	0.6512	0.0550
	LSTM	143.7693	80.9325	0.6439	0.0561
	GRU	173.80516	91.4636	0.6032	0.0723
Load	Informer	79.9029	62.6072	0.8084	0.0375
	Transformer	90.5427	69.5337	0.7748	0.0487
	LSTM	85.8634	67.9785	0.7327	0.0436
	GRU	98.9743	75.9742	0.7859	0.0695

distribution system located in Guizhou Province, China, which contains a high proportion of renewable resources. The equivalent 11-node power grid topology is shown in Figure 4. In Figure 4, node 6 and node 11 are equipped with 2.6 MW and 2.05 MW photovoltaic power stations, node 8 is equipped with 400 kW energy storage, nodes 1,3 and 5 are equipped with electric vehicle loads with a maximum capacity of 10% of the local load, and the power flow controller installed between nodes 9 and 11 has a capacity of 100 kW. The prediction part of the active support capability assessment model receives the historical series data from the rural power distribution system, including the output data of the photovoltaic power station, the node power load data, and the meteorological data required for prediction, with a period of March 2023 to September 2023 and a time granularity of 15 min.

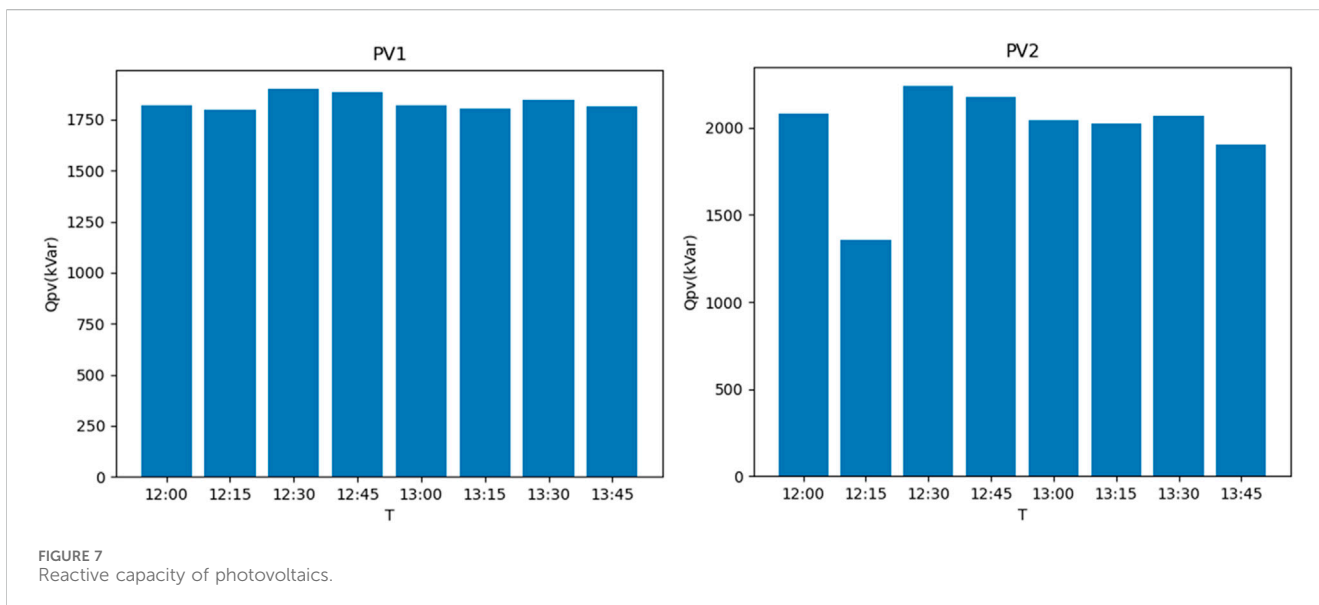
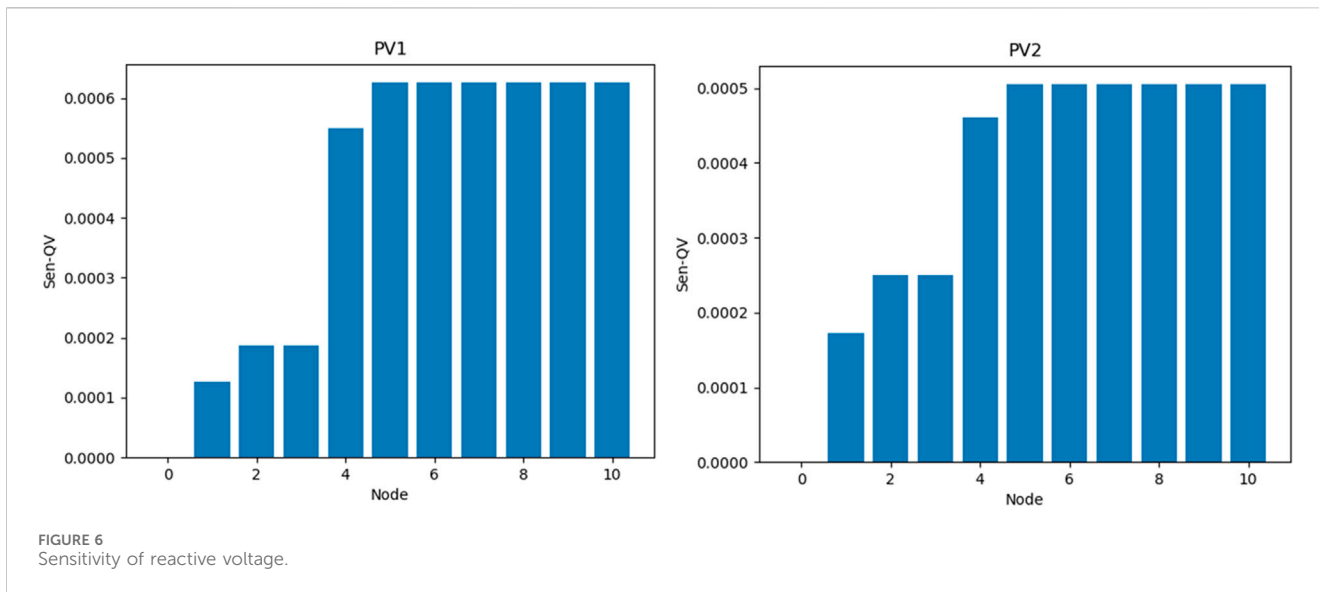
## 5.2 Evaluation of active support capability

Figure 5; Tables 1, 2 show the prediction results of the Informer model proposed in Section 2 for distributed photovoltaic and node power load in the region in the next 24 h and then quantitatively evaluate the active power support capacity of the rural power distribution system based on the prediction results. The predicted results in Figure 5 are obviously in line with the trend of photovoltaic

## 5 Case studies

### 5.1 System data

The proposed active-reactive power collaborative optimization scheduling algorithm was tested in a rural



output and power load change over time. The difference between the predicted point value and the actual value is small, and both are within the range of the interval prediction, achieving the expected effect. In the evaluation and calculation part, with maximum/minimum range and maximum fluctuation range as key indicators, 18 sets of data are calculated in Table 1 to measure the volatility and stability of power data. At the same time, root mean square error (RMSE) and absolute error (MAE) are introduced as evaluation indexes for the accuracy of point prediction results. Prediction interval coverage (PIPC) and normalized average width of prediction interval (PINAW) are selected as evaluation indexes for the accuracy of interval prediction results. The comparison results are shown in Table 2. Compared with Transformer (Tian et al., 2022), LSTM (Zhang et al., 2024c), and GRU (Liu et al., 2022b), the distributed photovoltaic and power load forecasting model based on informer has better prediction effects in all aspects and can better improve the prediction accuracy of time series.

Figure 6 shows the reactive voltage support of two photovoltaic power stations located at node 6 and node 11 for the overall rural power distribution system when the photovoltaic power output is large at noon. It can be seen that when the reactive power output of the photovoltaic power station increases (Wang et al., 2023c), the voltage of other nodes will be affected and will rise accordingly, and the node closer to the photovoltaic power station is more sensitive to the change of photovoltaic reactive power output, and the voltage rise is also higher.

The changes in the adjustable reactive power capacity of the two photovoltaic power stations at 12–14 are shown in Figure 7. It can be seen from the figure that the adjustable reactive power capacity of the photovoltaic power station will decrease with the increase of the active power output (Cao et al., 2024). When it is at night, the active power output of the photovoltaic power station is almost 0, and the adjustable reactive power capacity is close to the installed capacity of the photovoltaic power station.

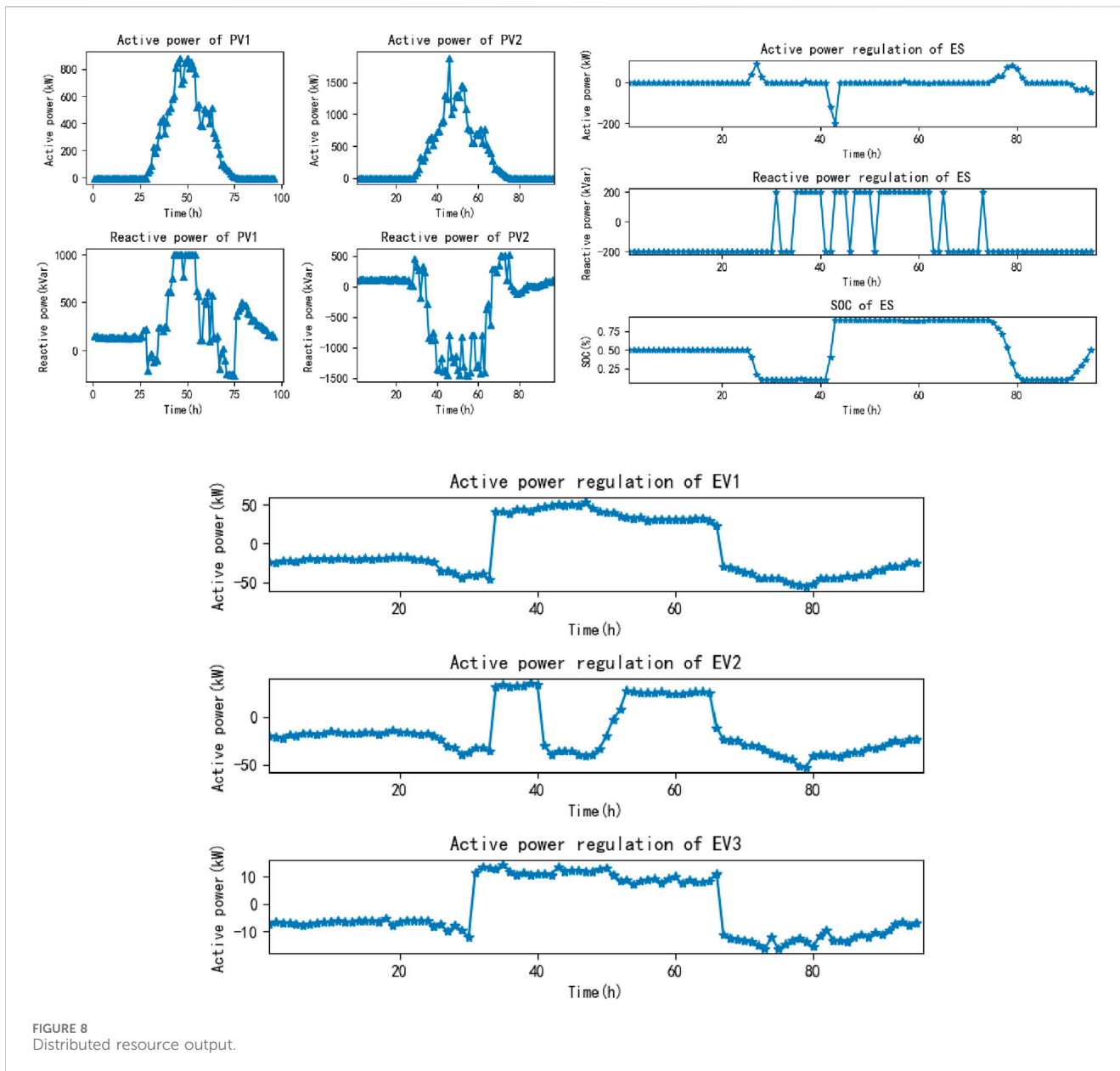


FIGURE 8 Distributed resource output.

### 5.3 Active-reactive power collaborative optimization scheduling

Based on the forecast results of distributed photovoltaic output and node power load for a total of 96 points in the next 24 h based on the Informer model, the day-ahead optimal scheduling was carried out by comprehensively considering the photovoltaic, energy storage, power flow controller and electric vehicle loads in the distribution system. The output curve of distributed photovoltaic, the operation curve of energy storage, and the load control curve of electric vehicles are shown in Figure 8. It can be seen that photovoltaics have no active power output at night and before sunrise, and only reactive power participates in system scheduling. In addition, when photovoltaic is generated, energy storage absorbs redundant active power, SOC increases significantly, and stops charging when rated capacity is reached.

The electric vehicle load also absorbs excess active power by increasing the load. As the sun goes down, the photovoltaic active power output is reduced. When the system has an energy gap, the energy storage and the electric vehicle load discharge to supplement the missing active power of the system.

Figure 9 shows the load distribution curve of the power distribution system as a whole and the change curve of the balance node (access point of the upper power grid). It can be observed that as time changes, the load of the two nodes where photovoltaics is located presents a trend of first increasing and then decreasing, when the photovoltaic output is insufficient, the system purchases electricity from the upper power grid through the balance node to meet the load demand, and when the photovoltaic output is too much, the redundant electricity is returned to the upper power grid, which is in line with the actual situation.

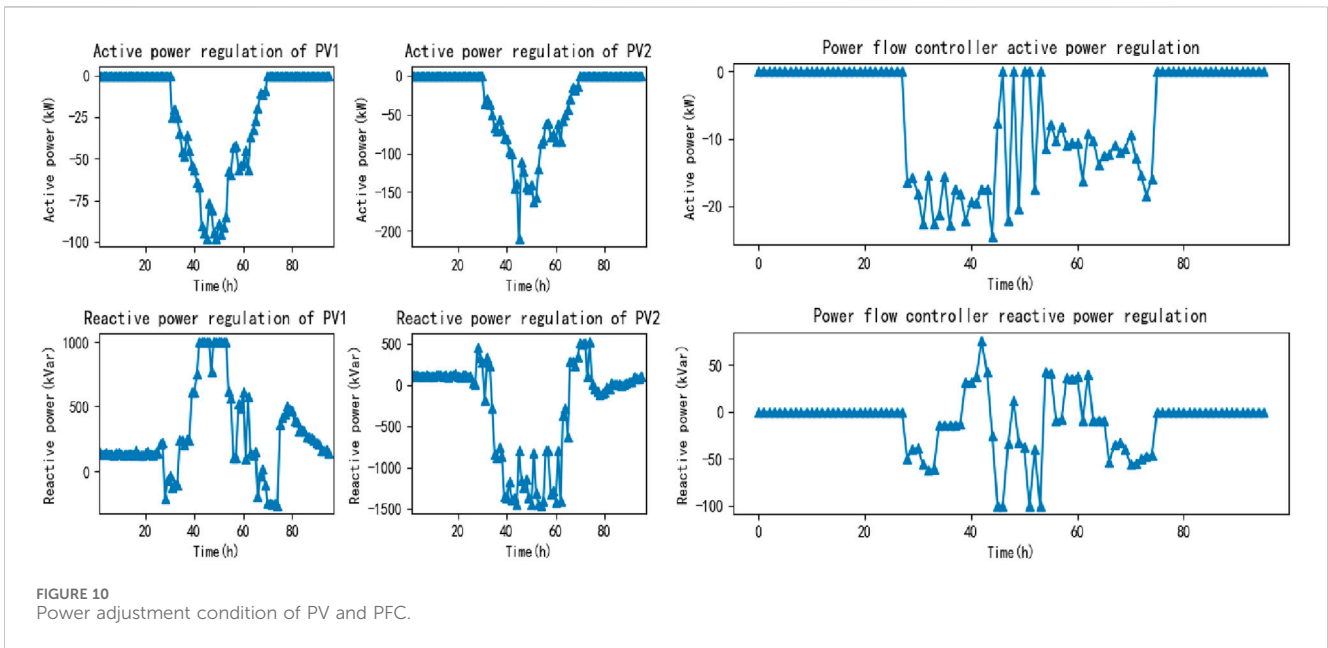
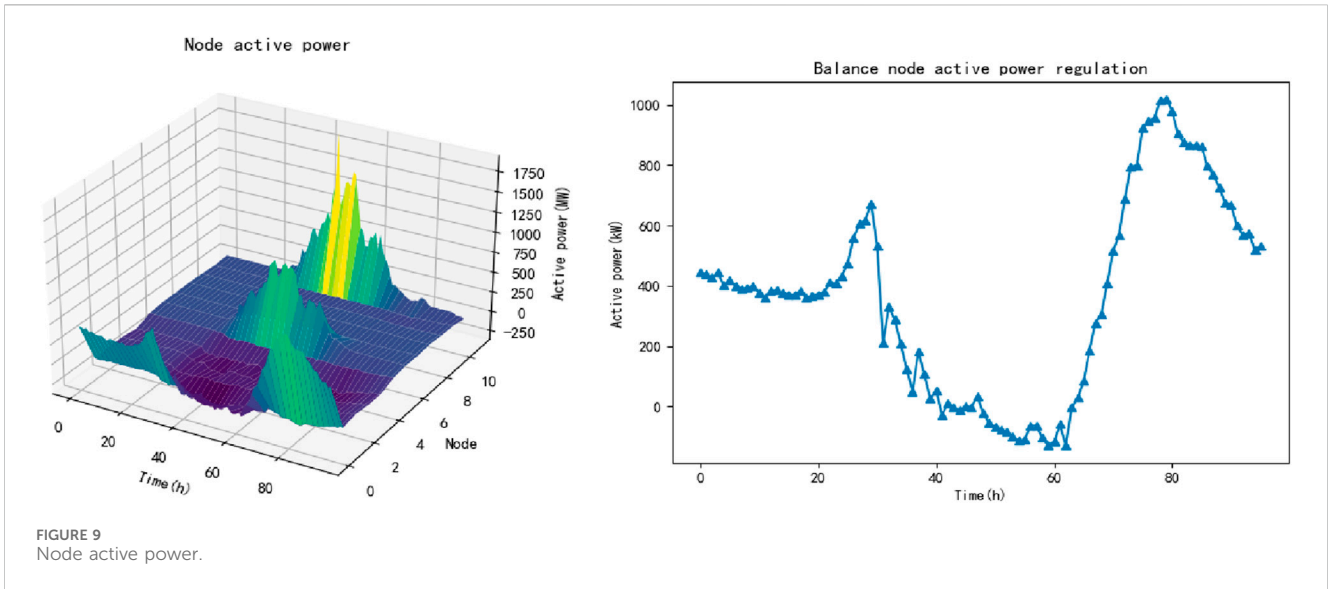


Figure 10 shows the adjustment amount of photovoltaic active/reactive power output and the change amount of electric vehicle load after the active-reactive power collaborative optimization scheduling. To ensure that the voltage of the nodes in the system does not exceed the limit when the photovoltaic power is generated, it is necessary to control the photovoltaic field station to reduce part of the active power output and guide the power flow controller to channel the line power flow. It can be found that with the changes in photovoltaic active power output and node load demand, the power flow controller can adjust the active and reactive power distribution of the line to ensure that the line voltage does not exceed the limit, and at the same time, it can reduce the amount of light discarded by photovoltaic, and effectively improve the absorption rate of renewable energy.

Figure 11; Table 3 compare the overall voltage and comprehensive cost of the rural power distribution system before and after optimization and regulation. By comparison, it can be seen that before optimizing and regulating the rural power distribution system, when the photovoltaic output is excess, the overall voltage of the system will exceed the upper limit, and when the photovoltaic output is insufficient, the overall voltage of the system maybe exceed the lower limit, which will bring serious harm to the power grid, and after optimized control, the node voltage is limited to a reasonable range, and the voltage fluctuation amplitude is significantly reduced.

In summary, two schemes are performed for comparisons to demonstrate the effectiveness and superiority of the proposed active-reactive power collaborative optimization scheduling: Compared to before collaborative scheduling, after collaborative scheduling, the comprehensive cost, including power-loss cost  $f_1$ ,

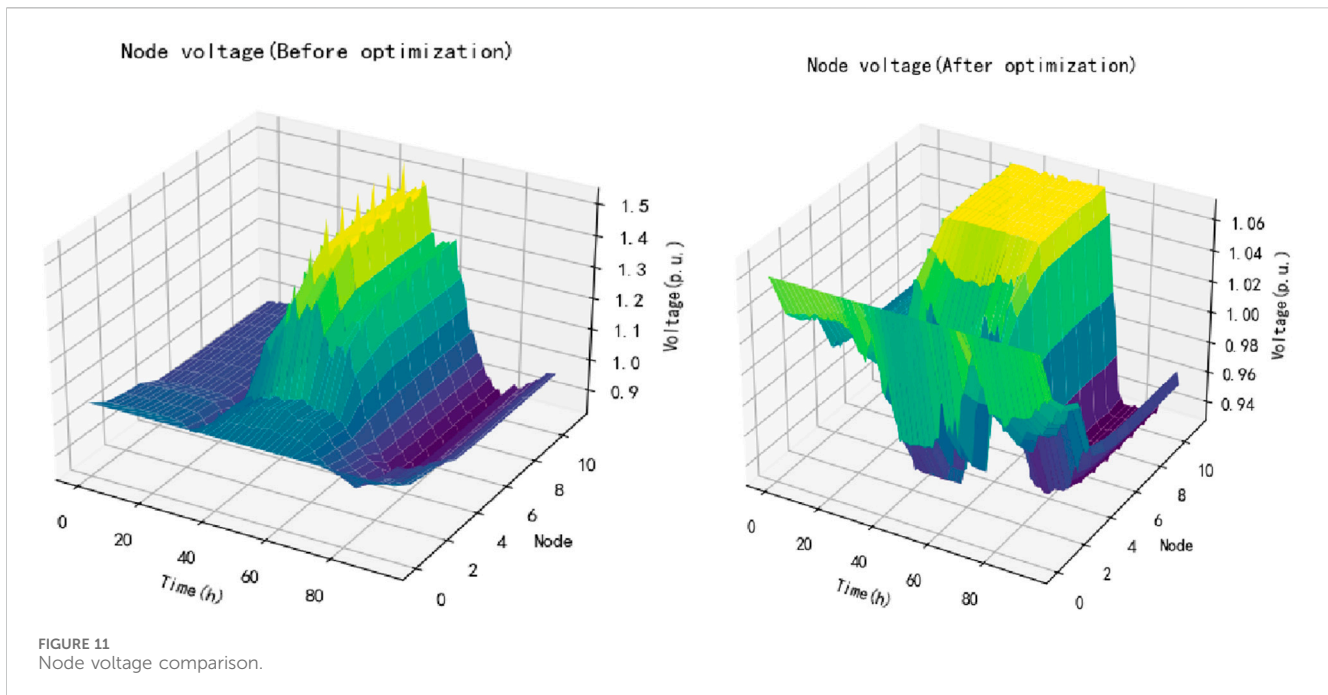


TABLE 3 Total cost comparison.

	Network loss cost	Operating cost	Penalty cost	Total cost
Before optimization	3,954.44	894.62	0	4,849.06
After optimization	3,219.40	792.85	324.61	4,336.86

distribution network operation cost  $f_2$ , and penalty cost  $f_3$ , is also lower, which is reduced by about 11.81%, and in order to meet the safe operation requirements of the distribution system, the overall photovoltaic active power output is reduced by about 6.86%, and by adjusting the output of distributed resources such as photovoltaic, the voltage of all load nodes at any time is limited to the safety standard, the maximum voltage reduction of the rural distribution system is approximately 27.2%. After optimized by the collaborative scheduling method, it not only meets the security of the power grid but also improves the economy. Therefore, the active-reactive power collaborative optimization scheduling method proposed in this paper has obvious advantages and can carry out reasonable and efficient optimization and regulation of this kind of rural power distribution system.

## 6 Conclusion

In order to solve the instability of rural power distribution systems with a high proportion of renewable energy, a method of active-reactive power collaborative optimization scheduling for rural power distribution systems is proposed. The key innovations proposed in this paper are as follows: 1) The quantitative evaluation indexes of active power support capability and reactive power support capability were put forward, and the evaluation model of active power support capability was established. The proposed evaluation model can more

accurately evaluate and quantify the support capacity of distributed resources for rural power distribution systems. Moreover, the accuracy of active power prediction based on informant model is about 13.26% higher than that of other methods mentioned in this paper; 2) The active-reactive power collaborative optimization scheduling model for rural power distribution systems with a high proportion of renewable energy was established, which greatly improved the safety and economy of the distribution system compared with the non-optimization, the comprehensive cost could be reduced by about 11.81%, and the maximum voltage reduction of the rural distribution system is approximately 27.2%; 3) The active support capability evaluation and regulation platform of the rural power distribution system is built to realize the active support capability evaluation of distributed resources and the scheduling control function of the new power distribution system, providing technical support services for the safe and stable operation of the rural power distribution system. In general, these innovations help to promote the safe, economic and stable operation of rural power distribution systems with a high proportion of renewable energy, and promote the construction of new rural power distribution systems.

## Data availability statement

The datasets presented in this article are not readily available because the dataset is from the electric power research institute of

Guizhou electric power grid, which is confidential. Requests to access the datasets should be directed to x15823764526@163.

## Author contributions

AL: Writing—original draft. XL: Data curation, Formal Analysis, Writing—review and editing. YL: Conceptualization, Methodology, Writing—review and editing. SH: Formal Analysis, Funding acquisition, Writing—review and editing. YM: Software, Supervision, Writing—review and editing. YZ: Conceptualization, Software, Writing—review and editing. JX: Data curation, Methodology, Writing—review and editing. QY: Supervision, Writing—review and editing, Methodology.

## Funding

The author(s) declare that financial support was received for the research, authorship, and/or publication of this article. This work was supported by the Science and Technology Project of Guizhou Power Grid under Grant GZKJXM20222149.

## References

- Akinyemi, A. S., Musasa, K., and Davidson, I. E. (2022). Analysis of voltage rise phenomena in electrical power network with high concentration of renewable distributed generations. *Sci. Rep.* 12 (7815), 7815. doi:10.1038/s41598-022-11765-w
- Albatsh, F. M., Mekhilef, S., Ahmad, S., and Mokhlis, H. (2017). Fuzzylogic-based UPFC and laboratory prototype validation for dynamic power flow control in transmission lines. *IEEE Trans. Ind. Electron.* 64 (12), 9538–9548. doi:10.1109/tie.2017.2711546
- Almeida, D., Pasupuleti, J., Raveendran, S. K., and Basir Khan, M. R. (2021). Performance evaluation of solar PV inverter controls for overvoltage mitigation in MV distribution networks. *Electronics* 10 (12), 1456. doi:10.3390/electronics10121456
- Babbar, S. M., Lau, C. Y., and Thang, K. F. (2021). Long term solar power generation prediction using adaboost as a hybrid of linear and non-linear machine learning model. *Int. J. Adv. Comput. S. C.* 12 (11), 546–545. doi:10.14569/ijacs.2021.0121161
- Cao, Y., Zhou, B., Chung, C. Y., Wu, T., Ling, Z., and Shuai, Z. (2024). A coordinated emergency response scheme for electricity and watershed networks considering spatio-temporal heterogeneity and volatility of rainstorm disasters. *IEEE Trans. Smart. Grid., Feb.* 1. doi:10.1109/TSG.2024.3362344
- Chawda, G. S., and Shaik, A. G. (2022). Enhancement of wind energy penetration levels in rural grid using ADALINE-LMS controlled distribution static compensator. *IEEE Trans. Sustain. Energy* 13 (1), 135–145. doi:10.1109/tste.2021.3105423
- Fu, X., and Zhou, Y. (2023). Collaborative optimization of PV greenhouses and clean energy systems in rural areas. *IEEE Trans. Sustain. Energy* 14 (1), 642–656. doi:10.1109/tste.2022.3223684
- Gao, H. J., Liu, J. Y., and Wang, L. F. (2018). Robust coordinated optimization of active and reactive power in active distribution systems. *IEEE Trans. Smart. Grid* 9 (5), 4436–4447. doi:10.1109/tsg.2017.2657782
- Gao, X. M., Yang, S. F., and Pan, S. B. (2017). Optimal parameter selection for support vector machine based on artificial bee colony algorithm: a case study of grid-connected pv system power prediction. *Comput. Intell. Neurosci.* 2017, 1–14. doi:10.1155/2017/7273017
- Han, J. S., Zhang, L., and Yang, L. (2022). Spatiotemporal analysis of rural energy transition and upgrading in developing countries: the case of China. *Appl. Energy* 307, 118225. doi:10.1016/j.apenergy.2021.118225
- Hou, C. F., Zhang, C. X., Wang, P., and Liu, S. (2024). Renewable energy based low-voltage distribution network for dynamic voltage regulation. *Results Eng.* 21, 101701. doi:10.1016/j.rineng.2023.101701
- Huang, Z. H., Zhang, Y. H., and Xie, S. W. (2022). Data-adaptive robust coordinated optimization of dynamic active and reactive power flow in active distribution networks. *Renew. Energy* 188, 164–183. doi:10.1016/j.renene.2022.02.027
- Jiang, T., Dong, X., Zhang, R., Li, X., Chen, H., and Li, G. (2023a). Active-reactive power scheduling of integrated electricity-gas network with multi-microgrids. *Front. Energy* 17, 251–265. doi:10.1007/s11708-022-0857-1
- Jiang, Y., Fu, K., Huang, W., Zhang, J., Li, X., and Liu, S. (2023b). “Ultra-short-term PV power prediction based on Informer with multi-head probability sparse self-attention mechanism”, *Front. Energy Res.*, vol. 11, pp. 1301828, doi:10.3389/fenrg.2023.1301828
- Kharrazi, A., Sreeram, V., and Mishra, Y. (2020). Assessment techniques of the impact of grid-tied rooftop photovoltaic generation on the power quality of low voltage distribution network - a review. *Renew. Sust. Energy Rev.* 120, 109643. doi:10.1016/j.rser.2019.109643
- Li, P., Zhang, C. C., Fu, X. P., Song, G., Wang, C., and Wu, J. (2019). Determination of local voltage control strategy of distributed generators in active distribution networks based on kriging metamodel. *IEEE Access* 7, 34438–34450. doi:10.1109/access.2019.2904144
- Liu, F., Zhang, Z., and Zhou, R. (2022b). Automatic modulation recognition based on CNN and GRU. *Tsinghua Sci. Technol.* 27 (2), 422–431. doi:10.26599/tst.2020.9010057
- Liu, X. J., Du, Z. B., Tan, Y. F., and Liu, Y. (2022a). Voltage optimization control strategy for islanded microgrid source-grid-load active-reactive power coordination based on collaborative Di-MPC. *Front. Energy Res.* 10, 880825. doi:10.3389/fenrg.2022.880825
- Osama abed el-Raouf, M., Mageed, S. A. A., Salama, M. M., Mosaad, M. I., and AbdelHadi, H. A. (2023). Performance enhancement of grid-connected renewable energy systems using UPFC. *Energies* 16 (11), 4362. doi:10.3390/en16114362
- Ru, N., Zhang, Z., and Zhang, H. (2021). “Carbon emission peak and carbon neutrality under the new target and vision,” in 2021 International Conference on Advanced Electrical Equipment and Reliable Operation (AEERO), Beijing, China, 15–17 Oct. 2021 (AEERO), 1–5.
- Tian, Z., Yi, J., Tao, J., Zhang, S., and Wen, Z. (2022). Hybrid autoregressive and non-autoregressive transformer models for speech recognition. *IEEE Signal Process* 29, 762–766. doi:10.1109/lsp.2022.3152128
- Wang, C. F., Wang, Y. L., Zhao, Y. J., Shuai, J., Shuai, C., and Cheng, X. (2023a). Cognition process and influencing factors of rural residents’ adoption willingness for solar PV poverty alleviation projects: evidence from a mixed methodology in rural China. *Energy* 271, 127078. doi:10.1016/j.energy.2023.127078
- Wang, J., Chen, L., Tan, Z., Du, E., Liu, N., Ma, J., et al. (2023b). Inherent spatiotemporal uncertainty of renewable power in China. *Nat. Commun.* 14, 5379. doi:10.1038/s41467-023-40670-7
- Wang, J., Gao, F., Zhou, Y., Guo, Q., Tan, C. W., Song, J., et al. (2023c). Data sharing in energy systems. *Adv. Appl. Energy* 10, 100132. doi:10.1016/j.adapen.2023.100132

## Conflict of interest

Authors AL, XL, YL, SH, YM, and YZ were employed by Electric Power Research Institute of Guizhou Electric Power Grid Co., Ltd. The remaining authors declare that the research was conducted in the absence of any commercial or financial relationships that could be construed as a potential conflict of interest.

The authors declare that this study received funding from the Science and Technology Project of Guizhou Power Grid. The funders had the following involvement in the study: the funders played an active role in research design, data collection and analysis, and decision to publish the manuscript.

## Publisher’s note

All claims expressed in this article are solely those of the authors and do not necessarily represent those of their affiliated organizations, or those of the publisher, the editors and the reviewers. Any product that may be evaluated in this article, or claim that may be made by its manufacturer, is not guaranteed or endorsed by the publisher.

- Wu, A., Ma, Z., Zeng, G., et al. (2011). Multi-layer cloud model for statistically analysis on renewable energy status in China's rural areas. *Chin. J. Electron* 20 (1), 101–104.
- Wu, X., Wang, R., Wang, Y., and Wang, L. (2022). A novel UPFC model and its convexification for security-constrained economic dispatch. *IEEE Trans. Power Syst.* 37 (6), 4202–4213. doi:10.1109/tpwrs.2022.3148090
- Xiao, C. L., Ding, M., Sun, L., and Chung, C. (2021). Network partition-based two-layer optimal scheduling for active distribution networks with multiple stakeholders. *IEEE Trans. Ind. Inf.* 17 (9), 5948–5960. doi:10.1109/tii.2020.3038668
- Xu, X., Zhang, T., Qiu, Z. W., Gao, H., Yu, H., Ma, Z., et al. (2024). Multi-mode control of a hybrid transformer for the coordinated regulation of voltage and reverse power in active distribution network. *Processes* 12 (2), 265. doi:10.3390/pr12020265
- Zhang, K., Luo, Y., Fu, Y., and Liu, N. (2024c). A hierarchical multi-timeframe multi-energy sharing framework for a self-sustained energy-transportation nexus. *IEEE Trans. Ind. Appl.* 60 (1), 1034–1047. doi:10.1109/tia.2023.3298870
- Zhang, K., Zuo, P., Zou, Z., Feng, X., Huang, Y., Wang, S., et al. (2024b). Forecasting medium-term F10.7 using the deep-learning informer model. *Sol. Phys.* 299 (47), 47. doi:10.1007/s11207-024-02284-0
- Zhang, K. Z., Xu, Y. L., and Sun, H. B. (2024a). Bilevel optimal coordination of active distribution network and charging stations considering EV drivers' willingness. *Appl. Energy* 360, 122790. doi:10.1016/j.apenergy.2024.122790
- Zhou, C. N., Xiong, B., Xue, H. Q., Zheng, D., Ge, Z., Wang, Y., et al. (2021). The role of new energy in carbon neutral. *Petroleum Explor. Dev.* 48 (2), 480–491. doi:10.1016/s1876-3804(21)60039-3
- Zhou, H. X., J Zhang, Y., Yang, L. F., Liu, Q., Yan, K., and Du, Y. (2019). Short-term photovoltaic power forecasting based on long short term memory neural network and attention mechanism. *IEEE Access* 7, 78063–78074. doi:10.1109/access.2019.2923006
- Zhuang, W., Fan, J. L., Xia, M., and Zhu, K. (2023). A multi-scale spatial-temporal graph neural network-based method of multienergy load forecasting in integrated energy system. *IEEE Trans. Smart Grid* 15, 2652–2666. doi:10.1109/tsg.2023.3315750
- Zhuang, W., Li, Z., Wang, Y., Xi, Q., and Xia, M. GCN-informer: a novel framework for mid-term photovoltaic power forecasting. *Appl. Sci.*, 2024; vol. 14, no. 5, pp. 2181, doi:10.3390/app14052181